Available online at www.sciencedirect.com
SCIENCE DIRECT®

Journal of Molecular Spectroscopy 237 (2006) 115–122

Journal of MOLECULAR SPECTROSCOPY

www.elsevier.com/locate/jms

# Spectrum of hot water in the 2000–4750 $cm^{-1}$ frequency range

Nikolai F. Zobov [a,1], Sergei V. Shirin [a,1], Oleg L. Polyansky [b,1], Robert J. Barber [a], Jonathan Tennyson [a,*], Pierre-François Coheur [c,2], Peter F. Bernath [d,e], Michel Carleer [c], Reginald Colin [c]

[a] Department of Physics and Astronomy, University College London, London, WC1E 6BT, UK
[b] Arbeitsgruppe Chemieinformationssysteme, Albert-Einstein-Allee 47, Ulm University, Ulm, Germany
[c] Université Libre de Bruxelles, Service de Chimie Quantique et Photophysique, 50 Av. F.D. Roosevelt, B-1050 Bruxelles, Belgium
[d] Department of Chemistry, University of Waterloo, Waterloo, Ont., Canada N2L 3G1
[e] Department of Chemistry, University of Arizona, Tucson, AZ 85721, USA

Received 4 February 2006
Available online 6 March 2006

**Abstract**

An emission spectrum recorded in an oxyacetylene torch [P.-F. Coheur, P.F. Bernath, M. Carleer, R. Colin, O.L. Polyansky, N.F. Zobov, S.V. Shirin, R.J. Barber, J. Tennyson, J. Chem. Phys. 122 (2005) 074307] is analyzed for the region covering stretching fundamentals and associated hot bands of water. Many lines could be assigned on the basis of previously determined energy levels. New assignments made with a new variational linelist allow a further 800 energy levels covering 15 vibrational states and rotations up to $J = 32$ to be assigned. A simultaneous re-analysis of previously reported sunspot absorption spectra leads to the assignment of 581 further lines in the *L*-band spectrum and 67 in the *N*-band spectrum.


*Keywords:* Water vapor; Line assignments; Sunspots

## 1. Introduction

The spectroscopy of water vapor finds application in a wide variety of areas including combustion science, atmospheric remote sensing, and astronomy [1]. In particular, hot water vapor is a prominent contributor to the spectral energy distributions of late M dwarf stars [2] and large sunspots [3,4]. These astronomical objects have effective temperatures of about 3000 K. The acquisition and interpretation of laboratory spectra of water vapor at 3000 K are therefore required for the calculation of molecular opacities [5] that are used to simulate these astronomical spectra. In fact the required molecular opacities are probably best calculated from some combination of energy levels and line intensities obtained from experiment with the predictions of state-of-the-art quantum chemistry [6].

The first modern high resolution spectra of hot water vapor were recorded by Maillard at the Meudon Observatory in France. He recorded emission spectra of an oxy-acetylene torch with a Fourier transform spectrometer and the analysis of these spectra was an important landmark in the spectroscopy of water vapor [7,8]. The advantage of the oxy-acetylene torch is that it produces a spectrum of water vapor at 3000 K, although the lines are nearly 0.1 $cm^{-1}$ wide primarily due to pressure-broadening at ambient atmospheric pressure. We have repeated the Maillard torch emission experiment and obtained new data over a wider spectral range and with somewhat higher signal-to-noise ratio. In our first paper based on these new data [9], we reported on the analysis of the pure rotation and $\nu_2$ bending mode region, 500–2000 $cm^{-1}$. The bending mode region yielded energy levels up to $9\nu_2$, which is over

* Corresponding author. Fax: +44 20 7679 7145.
*E-mail address:* j.tennyson@ucl.ac.uk (J. Tennyson).
[1] Permanent address: Institute of Applied Physics, Russian Academy of Science, Uljanov Street 46, Nizhnii Novgorod, Russia 603950.
[2] Research Associate with the F.N.R.S. (Belgium).

0022-2852/$ - see front matter © 2006 Elsevier Inc. All rights reserved.
doi:10.1016/j.jms.2006.03.001

the barrier to linearity and provided evidence for "monodromy" [10]. In the work reported below, we extend our analysis to the $\nu_1$ and $\nu_3$ stretching mode region, 2000–4750 $cm^{-1}$.

## 2. Observed spectra

The laboratory spectra reported by Coheur et al. [9] were obtained by recording emission from an oxy-acetylene torch using a Bruker IFS 120 M Fourier transform spectrometer between 500 and 13 000 $cm^{-1}$. In the region considered here (2000–4750 $cm^{-1}$) an InSb detector was used with a $CaF_2$ window and beamsplitter. Either a 2 or a 4 mm aperture was chosen and the spectral resolution was set to 0.05 $cm^{-1}$ (18 cm maximum optical path difference). Five hundred and twelve scans were co-added, thereby producing emission spectra with very low noise. Spectra were recorded with the torch at atmospheric pressure which, combined with a temperature of about 3000 K, leads to broadened lines with many blends and an uncertainty of about 0.02 $cm^{-1}$ in the determination of line positions. A few lines have fitting errors larger than this value; information on this is given in the archived version of the spectrum.

As is obvious from Fig. 1, the spectra are very dense, showing, in addition to water lines, emission features of CO, $CO_2$ and OH. The OH lines were identified in the spectra by using the spectroscopic constants of Colin et al. [11]. Vibrational levels up to $v = 8$ were considered in the comparison, and very weak satellite lines were neglected. Frequencies of OH rotational transitions were taken from Mélen et al. [12]. CO lines were similarly identified by using the HITEMP database [13] as a reference, with $v = 8$ as the highest vibrational level, and both the $^{12}$CO and $^{13}$CO isotopes were considered. Many of the possible OH and CO lines identified in the spectrum and marked in the line list are likely due to water. These transitions match CO or OH line positions but only for transitions with higher vibrational or rotational quantum numbers than expected for a 3000 K source.

Carbon dioxide transitions form a major part of the spectrum: the region between 2200 and 2400 $cm^{-1}$ is dominated by $CO_2$ lines and was not analyzed. Outside this region $CO_2$ lines were identified using data taken from the carbon dioxide spectroscopic database (CDSD) system of the Institute of Atmospheric Optics of the Siberian Branch the Russian Academy of Sciences (see http://spectra.iao.ru).

15 229 lines were measured in the 2000–2200 and 2400–4750 $cm^{-1}$ regions, although, as discussed below, blends mean that these correspond to 19 008 transitions.

Two absorption spectra of sunspots [14] were reconsidered at the same time as the laboratory emission spectra. These sunspot spectra have an estimated water vapor temperature of 3200 K. The first covered the *L*-band (2497–3195 $cm^{-1}$), which had been previously analyzed [15], and contains 2723 lines of which 1207 have been assigned [15]. The second was the *N*-band spectrum spanning the 722–1011 $cm^{-1}$ region [3], which has also been partially analyzed before [4,9,10,16]. Obviously the *N*-band spectrum does not overlap the spectral regions considered here, but it is extremely rich and many of the new assignments made in the laboratory spectrum could be confirmed by transitions in *N*-band spectrum using predicted combination differences.

Fig. 1 compares a small portion of the laboratory emission spectrum with the sunspot absorption spectrum of Wallace et al. [14]. Table 1 presents the corresponding

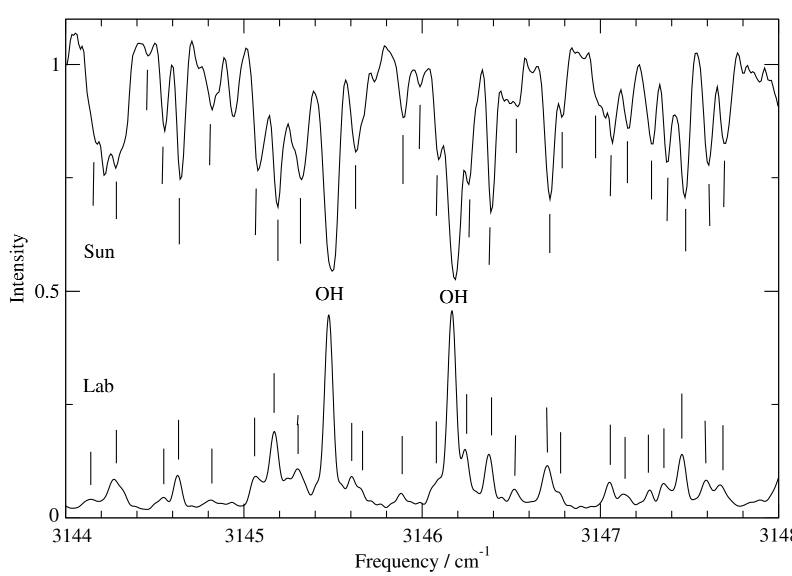


Fig. 1. Comparison of a sunspot absorption spectrum (upper trace) [14] and the laboratory emission spectrum (lower trace). The vertical lines indicate the location of assigned transitions as reported in Table 1. The vertical scale on the left refers to the sunspot absorption spectrum; the laboratory emission spectrum was not obtained on an absolute scale.

Table 1
Laboratory emission linelist in the region 3144–3148 $cm^{-1}$, corresponding to Fig. 1

| Wavenumber ($cm^{-1}$) | Peak height arb. units | $J'$ | $K'_a$ | $K'_c$ | $J''$ | $K''_a$ | $K''_c$ | $v'_1v'_2v'_3 - v''_1v''_2v''_3$ | Notes |
|---|---|---|---|---|---|---|---|---|---|
| 3144.15772 | 0.0166 | | | | | | | | OH |
| 3144.29116 | 0.0557 | 14 | 10 | 4 | 15 | 10 | 5 | 101 – 100 | dnc |
| 3144.55555 | 0.0217 | 9 | 0 | 9 | 10 | 0 | 10 | 300 – 101 | d |
| | | 9 | 1 | 8 | 10 | 3 | 7 | 022 – 021 | |
| 3144.64157 | 0.0721 | 22 | 3 | 20 | 23 | 3 | 21 | 002 – 001 | nc |
| | | 19 | 7 | 12 | 20 | 7 | 13 | 002 – 001 | |
| 3144.82506 | 0.0104 | 8 | 2 | 7 | 9 | 2 | 8 | 300 – 101 | |
| | | 9 | 3 | 7 | 10 | 3 | 8 | 211 – 210 | |
| 3144.93731 | 0.0132 | | | | | | | | |
| 3145.08231 | 0.0456 | 17 | 4 | 14 | 18 | 4 | 15 | 101 – 100 | |
| 3145.18235 | 0.1500 | 22 | 5 | 17 | 23 | 5 | 18 | 001 – 000 | |
| 3145.31097 | 0.0523 | 22 | 2 | 21 | 23 | 2 | 22 | 012 – 011 | nc |
| 3145.31097 | 0.0523 | 11 | 3 | 8 | 12 | 5 | 7 | 012 – 011 | |
| 3145.48902 | 0.4270 | | | | | | | | OH |
| 3145.61306 | 0.0345 | 15 | 6 | 9 | 16 | 5 | 12 | 030 – 010 | |
| | | 12 | 2 | 11 | 13 | 2 | 12 | 200 – 001 | |
| 3145.65105 | 0.0236 | 16 | 9 | 7 | 17 | 9 | 8 | 021 – 100 | n |
| | | 17 | 3 | 14 | 18 | 3 | 15 | 101 – 100 | |
| 3145.89319 | 0.0192 | 11 | 3 | 9 | 12 | 5 | 8 | 001 – 000 | |
| 3146.08289 | 0.0299 | 21 | 5 | 16 | 22 | 5 | 17 | 011 – 010 | |
| 3146.18003 | 0.4620 | | | | | | | | OH |
| 3146.25914 | 0.0779 | 24 | 1 | 24 | 25 | 1 | 25 | 002 – 001 | d |
| 3146.38747 | 0.1040 | 20 | 0 | 20 | 21 | 0 | 21 | 101 – 100 | d |
| | | 11 | 2 | 10 | 12 | 2 | 11 | 201 – 200 | |
| 3146.53177 | 0.0255 | 20 | 2 | 19 | 21 | 1 | 20 | 110 – 010 | |
| | | 14 | 5 | 9 | 15 | 6 | 10 | 100 – 000 | |
| 3146.71496 | 0.0861 | 16 | 5 | 11 | 17 | 5 | 12 | 101 – 100 | |
| 3146.78179 | 0.0242 | 20 | 7 | 14 | 21 | 7 | 15 | 011 – 010 | |
| | | 18 | 4 | 14 | 19 | 5 | 15 | 100 – 000 | |
| 3147.06398 | 0.0482 | 19 | 3 | 16 | 20 | 4 | 17 | 100 – 000 | nc |
| | | 24 | 1 | 24 | 25 | 1 | 25 | 031 – 030 | |
| 3147.14849 | 0.0214 | 21 | 4 | 18 | 22 | 4 | 19 | 002 – 001 | |
| 3147.28671 | 0.0332 | 24 | 0 | 24 | 25 | 0 | 25 | 031 – 030 | |
| 3147.37491 | 0.0400 | 15 | 5 | 11 | 16 | 5 | 12 | 111 – 110 | |
| 3147.46963 | 0.1040 | 21 | 3 | 18 | 22 | 3 | 19 | 002 – 001 | d |
| | | 25 | 1 | 25 | 26 | 1 | 26 | 021 – 020 | |
| 3147.60458 | 0.0494 | 20 | 5 | 15 | 21 | 5 | 16 | 021 – 020 | |
| | | 19 | 2 | 17 | 20 | 3 | 18 | 110 – 010 | |
| 3147.68407 | 0.0345 | 11 | 10 | 1 | 12 | 11 | 2 | 002 – 100 | dnc |

The notes mean: ‘n,’ new upper level; ‘c,’ confirmed by combination differences; ‘d,’ doublet due to degeneracy. Note the double assignment of many of the lines.

emission spectrum linelist for this small portion of the spectrum only. The full linelist as well as new versions of the sunspot spectra with updated assignments can be found in the electronic archive.

## 3. Line assignments

Line assignments were performed using the BT2 linelist [5]. This linelist was computed in order to model the spectrum of water vapor in cool stars and is thus suitable for the temperatures considered here. BT2 contains all transitions between levels of water with $J \leqslant 50$ and energy less than 30000 $cm^{-1}$ above the $J = 0$ ground state. Transition wavenumbers and wavefunctions were calculated using the spectroscopically determined potential energy surface of Shirin et al. [18]; transition intensities were obtained using the dipole moment surface of Schwenke and Partridge [19].

Table 2
Summary of new energy levels

| Vib. level | Number of new levels | Highest $J$ | |
|---|---|---|---|
| | | Prev. | This work |
| (100) | 62 | 30 | 36 |
| (001) | 65 | 32 | 37 |
| (110) | 80 | 27 | 32 |
| (011) | 28 | 30 | 35 |
| (120) | 31 | 20 | 23 |
| (021) | 25 | 30 | 32 |
| (200) | 74 | 19 | 29 |
| (101) | 37 | 28 | 29 |
| (002) | 137 | 26 | 32 |
| (130) | 15 | 14 | 14 |
| (031) | 36 | 25 | 29 |
| (111) | 16 | 26 | 22 |
| (012) | 55 | 20 | 29 |
| (041) | 15 | 25 | 25 |
| (121) | 20 | 15 | 20 |
| (022) | 19 | 19 | 26 |
| (131) | 14 | 11 | 22 |

Table 3
Newly assigned transitions in the sunspot $N$-band spectrum

| Wavenumber | $J'$ | $K'_a$ | $K'_c$ | $J''$ | $K''_a$ | $K''_c$ | $v'_1v'_2v'_3 - v''_1v''_2v''_3$ |
|---|---|---|---|---|---|---|---|
| 733.63047 | 20 | 7 | 13 | 19 | 6 | 14 | 021 − 021 |
| 738.78441 | 20 | 10 | 11 | 19 | 9 | 10 | 110 − 030 |
| 747.22399 | 20 | 7 | 13 | 19 | 6 | 14 | 031 − 031 |
| 760.93078 | 21 | 11 | 10 | 20 | 10 | 11 | 110 − 110 |
| 764.85815 | 19 | 6 | 14 | 18 | 6 | 13 | 021 − 040 |
| 767.36292 | 20 | 16 | 4 | 19 | 15 | 5 | 011 − 011 |
| 768.78462 | 14 | 6 | 9 | 13 | 3 | 10 | 120 − 120 |
| 774.16285 | 18 | 7 | 12 | 17 | 4 | 13 | 002 − 002 |
| 777.89056 | 24 | 10 | 15 | 23 | 9 | 14 | 100 − 020 |
| 778.32496 | 20 | 20 | 1 | 19 | 19 | 0 | 110 − 110 |
| 793.14810 | 20 | 5 | 16 | 19 | 10 | 9 | 120 − 030 |
| 797.86795 | 17 | 6 | 12 | 16 | 3 | 13 | 110 − 110 |
| 805.93601 | 16 | 8 | 9 | 15 | 7 | 8 | 200 − 040 |
| 809.74188 | 14 | 4 | 11 | 13 | 1 | 12 | 130 − 130 |
| 819.68444 | 22 | 16 | 7 | 21 | 15 | 6 | 110 − 110 |
| 820.86278 | 16 | 5 | 12 | 15 | 2 | 13 | 120 − 120 |
| 825.22767 | 22 | 18 | 5 | 21 | 17 | 4 | 110 − 110 |
| 826.31982 | 17 | 4 | 13 | 16 | 3 | 14 | 120 − 120 |
| 826.86678 | 17 | 3 | 14 | 16 | 2 | 15 | 002 − 002 |
| 827.50499 | 23 | 14 | 9 | 22 | 13 | 10 | 110 − 110 |
| 836.59448 | 15 | 3 | 13 | 14 | 0 | 14 | 110 − 110 |
| 837.15424 | 18 | 5 | 14 | 17 | 2 | 15 | 200 − 200 |
| 840.18222 | 23 | 16 | 7 | 22 | 15 | 8 | 110 − 110 |
| 840.94358 | 16 | 3 | 13 | 15 | 2 | 14 | 110 − 110 |
| 843.02101 | 24 | 17 | 7 | 23 | 16 | 8 | 001 − 001 |
| 843.96547 | 23 | 17 | 6 | 22 | 16 | 7 | 110 − 110 |
| 853.42384 | 20 | 8 | 13 | 19 | 7 | 12 | 110 − 030 |
| 854.06118 | 24 | 15 | 10 | 23 | 14 | 9 | 110 − 110 |
| 867.38053 | 25 | 18 | 8 | 24 | 17 | 7 | 001 − 001 |
| 871.75264 | 19 | 5 | 14 | 18 | 4 | 15 | 021 − 021 |
| 872.10943 | 22 | 8 | 15 | 21 | 7 | 14 | 110 − 030 |
| 875.49814 | 21 | 6 | 15 | 20 | 5 | 16 | 110 − 110 |
| 880.67718 | 19 | 4 | 15 | 18 | 3 | 16 | 002 − 002 |
| 883.57597 | 21 | 6 | 15 | 20 | 5 | 16 | 001 − 001 |
| 890.45791 | 26 | 19 | 7 | 25 | 18 | 8 | 001 − 001 |
| 896.91056 | 23 | 7 | 16 | 22 | 6 | 17 | 100 − 100 |
| 898.79726 | 23 | 8 | 16 | 24 | 9 | 15 | 020 − 010 |
| 901.01798 | 30 | 0 | 30 | 30 | 1 | 29 | 021 − 011 |
| 914.84521 | 29 | 1 | 29 | 29 | 2 | 28 | 021 − 011 |
| 916.47109 | 29 | 11 | 18 | 28 | 10 | 19 | 010 − 010 |
| 923.31000 | 19 | 6 | 14 | 18 | 3 | 15 | 021 − 021 |
| 926.75156 | 22 | 6 | 16 | 21 | 5 | 17 | 100 − 100 |
| 927.30019 | 21 | 5 | 16 | 20 | 4 | 17 | 002 − 002 |
| 931.85413 | 29 | 10 | 19 | 28 | 9 | 20 | 010 − 010 |
| 933.06676 | 22 | 6 | 16 | 21 | 5 | 17 | 020 − 020 |
| 934.69998 | 18 | 8 | 11 | 17 | 5 | 12 | 110 − 110 |
| 947.65682 | 19 | 6 | 14 | 20 | 8 | 13 | 021 − 030 |
| 950.33241 | 17 | 3 | 15 | 16 | 0 | 16 | 110 − 110 |
| 952.50148 | 17 | 3 | 14 | 16 | 2 | 15 | 120 − 120 |
| 954.56809 | 16 | 3 | 14 | 15 | 0 | 15 | 120 − 120 |
| 957.91102 | 22 | 6 | 16 | 21 | 5 | 17 | 021 − 021 |
| 960.31126 | 20 | 8 | 13 | 19 | 5 | 14 | 110 − 110 |
| 961.85750 | 27 | 19 | 8 | 26 | 18 | 9 | 020 − 020 |
| 962.20082 | 21 | 5 | 16 | 20 | 4 | 17 | 110 − 110 |
| 963.78980 | 31 | 1 | 31 | 31 | 2 | 30 | 011 − 001 |
| 965.80308 | 23 | 6 | 17 | 22 | 5 | 18 | 002 − 002 |
| 966.77900 | 23 | 8 | 16 | 22 | 5 | 17 | 100 − 100 |
| 968.56967 | 30 | 14 | 17 | 29 | 13 | 16 | 010 − 010 |
| 974.10225 | 16 | 5 | 12 | 17 | 6 | 11 | 120 − 110 |
| 975.26034 | 22 | 6 | 17 | 21 | 3 | 18 | 002 − 002 |
| 976.04084 | 22 | 10 | 13 | 23 | 11 | 12 | 110 − 100 |
| 976.74869 | 20 | 4 | 17 | 19 | 1 | 18 | 200 − 200 |
| 981.15597 | 30 | 1 | 30 | 30 | 2 | 29 | 110 − 100 |
| 986.31764 | 10 | 2 | 9 | 11 | 3 | 8 | 130 − 120 |

Table 3 (*continued*)

| Wavenumber | $J'$ | $K'_a$ | $K'_c$ | $J''$ | $K''_a$ | $K''_c$ | $v'_1v'_2v'_3 - v''_1v''_2v''_3$ |
|---|---|---|---|---|---|---|---|
| 988.17414 | 18 | 4 | 15 | 17 | 1 | 16 | 120 − 120 |
| 1008.38530 | 22 | 8 | 15 | 21 | 5 | 16 | 110 − 110 |
| 1010.06112 | 20 | 9 | 12 | 21 | 10 | 11 | 110 − 020 |

The first step in analyzing the torch spectrum was to mark transitions belonging to other species: we firmly identify 389 OH lines and 825 CO lines; a further 984 lines are identified as possibly belonging to OH or CO transitions. 1180 $CO_2$ lines are identified in 3400–3800 $cm^{-1}$ region.

The second step was to make trivial assignments—that is assignments that can be made using previously determined experimental energy levels [20]. Simple checks were made using the theoretical intensities to ensure that the intensity of each assigned transition was consistent with observation. It was possible to assign 12431 lines in this fashion. At this stage 2965 lines remained unassigned.

Two different methods were used to assign new lines. For transitions involving states with high $J$ but low $K_a$, the method of branches [16,21] was used to follow a series of transitions with quantum numbers which simply differ by one in $J$. This method was used for 18 low-lying vibrational levels and yielded about 300 new energy levels.

For transitions with $J$ in the range of 15–25 and intermediate values of $K_a$, the error (obs. – calc.) obtained using the BT2 predictions varies smoothly with $K_a$ and $K_c$. This means that the positions of experimentally determined energy levels could be predicted with sufficient accuracy for new assignments to be made. This method was used for 15 vibrational states associated with stretching transitions ($\Delta v_1$ or $\Delta v_3 = 1$) to yield about 500 new energy levels.

A copy of the assigned lines from the laboratory spectrum for the 2000–4750 $cm^{-1}$ region has been placed in the electronic archive. Table 2 summarizes the information obtained for the main vibrational states analyzed; there are a number of other vibrational states for which a few (less than 10) new levels were obtained. It can be seen that our analysis has extended the range of rotational excitation for a significant number of vibrational states. The greatest number of new energy levels belong to the (002) state; transitions involving this level appear to be under-represented in the analysis of previous hot water spectra.

Most of the transitions in the 2000–4750 $cm^{-1}$ region involve changes in one of the stretching quantum numbers, either $v_1$ or $v_3$, by one quantum. However, at higher wavenumbers there are also transitions which correspond to the P-branch of two quantum transitions involving a simultaneous change in a stretching quantum number and the bending quantum number $v_2$. It is to be expected that further transitions of this nature will be identified at higher frequencies.

Copies of the sunspot absorption spectra with our new assignments have also been placed in the electronic archive. The $L$-band spectrum contains only 2723 transitions as against 4593 in the torch emission spectrum in the same region and contains only a few new lines. New assignments to the sunspot spectrum were therefore largely taken from those made for the torch spectrum. This process resulted in the assignment of 1579 water transitions, 199 OH lines and 10 HCl lines; a total of 1788 assignments as opposed to the 1207 made previously [15].

The $N$-band sunspot spectrum is very dense [4,16] and the present study just focused on a few transitions which could be used to confirm assignments in the torch spectrum. As a result of this 67 new transitions were assigned; these are listed in Table 3.

Table 4 presents the new energy levels obtained from our analysis of the spectra discussed above. In this table, we concentrate on high rotational quantum numbers for which there is no previous information. We estimate the error for each of these levels to be about 0.02 $cm^{-1}$, similar to the error in determining the line positions in the laboratory emission spectrum. The table indicates the levels which have been confirmed by combination differences. The values for the other levels, which all rely on a single assigned transition, must be regarded as less secure. However, our experience has shown that the methods we employ are reliable and it is likely that the vast majority of these unconfirmed levels are also correct.

## 4. Discussion and conclusion

By the standards of modern Fourier transform spectroscopy, the oxy-acetylene torch produces spectra of only modest resolution because of the extensive pressure-broadening of the lines. In addition, Doppler-broadening also makes a contribution (0.09 $cm^{-1}$ at 10000 $cm^{-1}$ for 3000 K) to the typical linewidth of about 0.1 $cm^{-1}$ above 5000 $cm^{-1}$. Below 5000 $cm^{-1}$ our average linewidth is about 0.06 $cm^{-1}$ and nearly all of the lines are overlapped, see Table 1. The new BT2 linelist [5], however, predicts energy levels to between 0.2 and 0.4 $cm^{-1}$ for $J = 30$. However, there is considerable cancelation of errors for transition wavenumbers for which this error is more typically 0.1 $cm^{-1}$, a figure which can be very significantly reduced by employing the method of branches discussed above. Furthermore the BT2 linelist has reliable line intensities.

Although our new spectra cover a wider spectral range and have a better signal-to-noise ratio than the earlier Meudon spectra, it is the availability of the BT2 linelist that makes assignments possible. In the stretching mode region (2000–4750 $cm^{-1}$) covered in this paper, the torch spectra have provided extensive new highly exited vibration–rotation energy levels for more than a dozen vibrations (Table 2). In addition to the stretching fundamental (100) and (001), major improvements have been made to the vibrational levels that have two quanta of stretch, (002) and

Table 4
New energy levels, in $cm^{-1}$, for high $J$ vibration–rotation levels

| $J$ | $K_a$ | $K_c$ | Wavenumber |
|---|---|---|---|
| (100) | | | |
| 31 | 0 | 31 | 12748.5829 |
| 31 | 1 | 31 | 12748.5829 |
| 31 | 1 | 30 | 13291.7717 |
| 31 | 2 | 30 | 13291.7717 |
| 31 | 2 | 29 | 13759.1605 |
| 31 | 3 | 29 | 13759.1605 |
| 31 | 3 | 28 | 14198.9484 |
| 31 | 4 | 28 | 14198.9484 |
| 31 | 4 | 27 | 14601.7860 |
| 31 | 19 | 13 | 18848.7981 |
| 31 | 19 | 12 | 18848.7981 |
| 32 | 0 | 32 | 13310.1642 |
| 32 | 1 | 32 | 13310.1642 |
| 32 | 2 | 31 | 13870.8937 |
| 32 | 2 | 30 | 14346.0170 |
| 32 | 3 | 30 | 14346.0170 |
| 32 | 20 | 13 | 19848.2666 |
| 32 | 20 | 12 | 19848.2666 |
| 33 | 0 | 33 | 13887.1749 |
| 33 | 1 | 33 | 13887.1749 |
| 33 | 1 | 32 | 14462.3518 |
| 34 | 1 | 33 | 15070.5999 |
| 34 | 2 | 33 | 15070.5999 |
| 35 | 0 | 35 | 15086.5589 |
| 35 | 1 | 35 | 15086.5589 |
| 35 | 1 | 34 | 15694.1713 |
| 35 | 2 | 34 | 15694.1713 |
| 36 | 0 | 36 | 15708.5886 |
| 36 | 1 | 36 | 15708.5886 |
| (001) | | | |
| 32 | 2 | 30 | 14474.2885[a] |
| 32 | 3 | 30 | 14474.2885[a] |
| 32 | 3 | 29 | 14921.4139[a] |
| 32 | 4 | 29 | 14921.4139[a] |
| 32 | 5 | 27 | 15713.6124 |
| 32 | 6 | 27 | 15713.6124 |
| 33 | 0 | 33 | 14023.1636 |
| 33 | 1 | 33 | 14023.1636 |
| 33 | 1 | 32 | 14593.1539[a] |
| 33 | 2 | 32 | 14593.1539[a] |
| 33 | 2 | 31 | 15077.4570[a] |
| 33 | 3 | 31 | 15077.4570[a] |
| 33 | 3 | 30 | 15535.5755[a] |
| 33 | 4 | 30 | 15535.5755[a] |
| 34 | 0 | 34 | 14617.4624[a] |
| 34 | 1 | 34 | 14617.4624[a] |
| 34 | 1 | 33 | 15202.8292[a] |
| 34 | 2 | 33 | 15202.8292[a] |
| 34 | 2 | 32 | 15694.4241[a] |
| 34 | 3 | 32 | 15694.4241[a] |
| 34 | 3 | 31 | 16163.4249[a] |
| 34 | 4 | 31 | 16163.4249[a] |
| 34 | 4 | 30 | 16593.1373[a] |
| 34 | 5 | 30 | 16593.1373[a] |
| 35 | 0 | 35 | 15226.7754[a] |
| 35 | 1 | 35 | 15226.7754[a] |
| 35 | 2 | 34 | 15827.1128 |
| 35 | 3 | 32 | 16804.7609[a] |
| 35 | 4 | 32 | 16804.7609[a] |
| 36 | 0 | 36 | 15850.9489 |
| 36 | 1 | 36 | 15850.9489 |
| 36 | 1 | 35 | 16466.6258 |
| 36 | 2 | 35 | 16466.6258 |
| 36 | 2 | 34 | 16968.1804 |
| 36 | 3 | 34 | 16968.1804 |
| 37 | 0 | 37 | 16489.8206 |
| 37 | 1 | 37 | 16489.8206 |
| (110) | | | |
| 28 | 0 | 28 | 12671.4844 |
| 28 | 1 | 28 | 12671.4844 |
| 28 | 1 | 27 | 13246.5813 |
| 28 | 2 | 27 | 13246.5813 |
| 28 | 3 | 26 | 13699.4792 |
| 29 | 0 | 29 | 13182.9526 |
| 29 | 1 | 29 | 13182.9526 |
| 29 | 1 | 28 | 13773.7550 |
| 29 | 2 | 27 | 14239.5862 |
| 30 | 0 | 30 | 13710.5145[a] |
| 30 | 1 | 30 | 13710.5145[a] |
| 31 | 0 | 31 | 14254.0956 |
| 31 | 1 | 31 | 14254.0956 |
| 32 | 0 | 32 | 14813.9119 |
| 32 | 1 | 32 | 14813.9119 |
| (011) | | | |
| 31 | 0 | 31 | 14382.9537[a] |
| 31 | 1 | 31 | 14382.9537[a] |
| 31 | 1 | 30 | 15012.3386[a] |
| 31 | 2 | 30 | 15012.3386[a] |
| 32 | 0 | 32 | 14944.2833[a] |
| 32 | 1 | 32 | 14944.2833[a] |
| 33 | 0 | 33 | 15521.6588[a] |
| 33 | 1 | 33 | 15521.6588[a] |
| 33 | 2 | 32 | 16193.0260 |
| 34 | 0 | 34 | 16115.0888[a] |
| 34 | 1 | 34 | 16115.0888[a] |
| 35 | 0 | 35 | 16724.6749 |
| 35 | 1 | 35 | 16724.6749 |
| (120) | | | |
| 21 | 0 | 21 | 11064.3886[a] |
| 21 | 1 | 21 | 11064.3131 |
| 21 | 1 | 20 | 11549.3003[a] |
| 21 | 2 | 19 | 11933.5430[a] |
| 21 | 3 | 18 | 12286.4048[a] |
| 23 | 0 | 23 | 11868.6405 |
| 23 | 1 | 22 | 12404.6686 |
| 23 | 2 | 21 | 12812.5262 |
| (021) | | | |
| 32 | 0 | 32 | 16466.3895[a] |
| 32 | 1 | 32 | 16466.3895[a] |
| (200) | | | |
| 20 | 0 | 20 | 11097.5337[a] |
| 20 | 1 | 20 | 11097.5337[a] |
| 20 | 1 | 19 | 11448.4725[a] |
| 20 | 2 | 19 | 11448.4725[a] |
| 20 | 3 | 18 | 11763.8805[a] |
| 20 | 4 | 17 | 12048.7575[a] |
| 21 | 0 | 21 | 11473.2241[a] |
| 21 | 1 | 21 | 11473.2241[a] |
| 22 | 0 | 22 | 11865.4579 |
| 22 | 1 | 22 | 11865.4579 |
| 22 | 1 | 21 | 12250.8782 |
| 22 | 2 | 21 | 12250.8782 |
| 23 | 0 | 23 | 12274.1573[a] |
| 23 | 1 | 23 | 12274.1573[a] |

[a] Levels labeled have been confirmed by combination differences.

Table 4 (*continued*)

| $J$ | $K_a$ | $K_c$ | Wavenumber |
|---|---|---|---|
| 23 | 1 | 22 | 12676.5815[a] |
| 23 | 2 | 22 | 12676.5815[a] |
| 23 | 2 | 21 | 13037.8661[a] |
| 23 | 3 | 21 | 13037.8661[a] |
| 24 | 0 | 24 | 12699.1791[a] |
| 24 | 1 | 24 | 12699.1791[a] |
| 24 | 1 | 23 | 13118.5666[a] |
| 24 | 2 | 23 | 13118.5666[a] |
| 24 | 3 | 22 | 13494.2682[a] |
| 25 | 0 | 25 | 13140.3925[a] |
| 25 | 1 | 25 | 13140.3925[a] |
| 25 | 1 | 24 | 13576.6420 |
| 25 | 2 | 24 | 13576.6420 |
| 26 | 0 | 26 | 13597.6812 |
| 26 | 1 | 26 | 13597.6812 |
| 27 | 0 | 27 | 14070.9270[a] |
| 27 | 1 | 27 | 14070.9270[a] |
| 28 | 0 | 28 | 14559.8711 |
| 28 | 1 | 28 | 14559.8711 |
| 28 | 1 | 27 | 15046.4377 |
| 28 | 2 | 27 | 15046.4377 |
| 29 | 0 | 29 | 15064.2789 |
| 29 | 1 | 29 | 15064.2789 |
| (101) | | | |
| 29 | 0 | 29 | 15135.8316 |
| 29 | 1 | 29 | 15135.8316 |
| (002) | | | |
| 26 | 0 | 26 | 13881.7000[a] |
| 27 | 0 | 27 | 14358.0728[a] |
| 27 | 1 | 27 | 14358.1455 |
| 27 | 1 | 26 | 14821.0409 |
| 27 | 2 | 26 | 14821.0409 |
| 27 | 2 | 25 | 15233.3060[a] |
| 27 | 3 | 25 | 15233.3060[a] |
| 27 | 3 | 24 | 15611.2623 |
| 27 | 4 | 24 | 15611.2623 |
| 27 | 4 | 23 | 15958.1015[a] |
| 27 | 5 | 22 | 16276.3080 |
| 28 | 0 | 28 | 14850.2901[a] |
| 28 | 1 | 28 | 14850.2901[a] |
| 28 | 1 | 27 | 15329.2931[a] |
| 28 | 2 | 27 | 15329.2931[a] |
| 28 | 2 | 26 | 15753.5115 |
| 28 | 3 | 26 | 15753.5115 |
| 28 | 3 | 25 | 16144.2391[a] |
| 28 | 4 | 25 | 16144.2391[a] |
| 28 | 5 | 24 | 16503.1292 |
| 28 | 6 | 23 | 16832.8937 |
| 29 | 0 | 29 | 15358.2833[a] |
| 29 | 1 | 29 | 15358.2833[a] |
| 29 | 1 | 28 | 15853.1372[a] |
| 29 | 2 | 28 | 15853.1372[a] |
| 29 | 2 | 27 | 16288.6400[a] |
| 29 | 3 | 27 | 16288.6400[a] |
| 29 | 3 | 26 | 16691.8220 |
| 29 | 4 | 26 | 16691.8220 |
| 29 | 4 | 25 | 17062.0055 |
| 29 | 5 | 24 | 17402.3850 |
| 30 | 0 | 30 | 15881.9026[a] |
| 30 | 1 | 30 | 15881.9026[a] |
| 30 | 1 | 29 | 16392.4340 |
| 30 | 2 | 29 | 16392.4340 |
| 30 | 2 | 28 | 16838.5647 |
| 30 | 3 | 28 | 16838.5647 |

Table 4 (*continued*)

| $J$ | $K_a$ | $K_c$ | Wavenumber |
|---|---|---|---|
| 30 | 3 | 27 | 17253.8439[a] |
| 30 | 4 | 27 | 17253.8439[a] |
| 30 | 5 | 26 | 17635.1319 |
| 30 | 6 | 25 | 17988.9171 |
| 31 | 0 | 31 | 16420.9400[a] |
| 31 | 1 | 31 | 16420.9400[a] |
| 31 | 1 | 30 | 16947.0228 |
| 31 | 2 | 30 | 16947.0228 |
| 31 | 2 | 29 | 17403.1731 |
| 31 | 3 | 29 | 17403.1731 |
| 31 | 3 | 28 | 17830.0626 |
| 31 | 4 | 28 | 17830.0626 |
| 32 | 0 | 32 | 16975.0995 |
| 32 | 1 | 32 | 16975.0995 |
| 32 | 1 | 31 | 17516.7366 |
| 32 | 2 | 31 | 17516.7366 |
| (031) | | | |
| 26 | 0 | 26 | 14830.6603[a] |
| 26 | 1 | 26 | 14829.6624[a] |
| 26 | 2 | 24 | 15917.6825[a] |
| 27 | 1 | 27 | 15309.3848[a] |
| 27 | 2 | 26 | 16026.5598 |
| 28 | 0 | 28 | 15820.6570 |
| 28 | 1 | 27 | 16557.1781 |
| 29 | 1 | 29 | 16352.5276 |
| (012) | | | |
| 21 | 0 | 21 | 13261.9732[a] |
| 21 | 1 | 21 | 13261.9732[a] |
| 21 | 1 | 20 | 13673.3312[a] |
| 21 | 2 | 20 | 13673.3312[a] |
| 21 | 2 | 19 | 14035.5136 |
| 22 | 0 | 22 | 13652.9553[a] |
| 22 | 1 | 22 | 13652.9553[a] |
| 22 | 2 | 21 | 14084.4505[a] |
| 22 | 3 | 20 | 14459.5103[a] |
| 22 | 6 | 17 | 15359.8872[a] |
| 23 | 0 | 23 | 14060.3462[a] |
| 23 | 1 | 23 | 14060.3462[a] |
| 23 | 1 | 22 | 14512.0898[a] |
| 24 | 1 | 24 | 14484.1767[a] |
| 24 | 1 | 23 | 14956.0772[a] |
| 24 | 2 | 23 | 14956.0772[a] |
| 25 | 0 | 25 | 14924.4283[a] |
| 25 | 1 | 25 | 14924.4283[a] |
| 26 | 0 | 26 | 15380.3246[a] |
| 26 | 1 | 26 | 15380.3246[a] |
| 27 | 0 | 27 | 15852.6949[a] |
| 27 | 1 | 27 | 15852.6949[a] |
| 27 | 1 | 26 | 16385.8914[a] |
| 27 | 2 | 26 | 16385.8914[a] |
| 29 | 0 | 29 | 16845.3971[a] |
| 29 | 1 | 29 | 16845.3971[a] |
| (121) | | | |
| 16 | 0 | 16 | 12861.9997[a] |
| 16 | 1 | 16 | 12861.9970[a] |
| 16 | 1 | 15 | 13212.5809 |
| 16 | 2 | 14 | 13505.7941[a] |
| 16 | 3 | 13 | 13750.7322[a] |
| 17 | 0 | 17 | 13165.5455[a] |
| 17 | 1 | 17 | 13165.5455[a] |
| 17 | 2 | 16 | 13539.7452[a] |
| 18 | 1 | 17 | 13883.9766[a] |
| 18 | 2 | 16 | 14214.0400 |

(*continued on next page*)

Table 4 (*continued*)

| $J$ | $K_a$ | $K_c$ | Wavenumber |
|---|---|---|---|
| 19 | 1 | 19 | 13822.9574[a] |
| 19 | 3 | 17 | 14591.0213 |
| 19 | 4 | 16 | 14895.0345 |
| 20 | 0 | 20 | 14176.8775[a] |
| 20 | 1 | 20 | 14176.7528[a] |
| 20 | 2 | 19 | 14623.3093 |
| (022) | | | |
| 20 | 0 | 20 | 14382.9908[a] |
| 20 | 1 | 19 | 14826.6092[a] |
| 20 | 2 | 19 | 14826.6092[a] |
| 20 | 4 | 17 | 15515.4665[a] |
| 21 | 0 | 21 | 14754.5857[a] |
| 21 | 1 | 21 | 14754.6016[a] |
| 21 | 2 | 19 | 15601.3923[a] |
| 22 | 1 | 22 | 15142.9020[a] |
| 22 | 2 | 21 | 15634.2405 |
| 22 | 3 | 20 | 16025.9848 |
| 23 | 0 | 23 | 15547.2854[a] |
| 23 | 1 | 22 | 16063.6045[a] |
| 24 | 1 | 24 | 15968.9740[a] |
| 24 | 2 | 23 | 16509.3366[a] |
| 24 | 3 | 22 | 16924.5085[a] |
| 26 | 1 | 26 | 16861.4715 |
| (131) | | | |
| 13 | 1 | 13 | 13532.2929 |
| 13 | 3 | 11 | 14103.3813 |
| 13 | 4 | 10 | 14325.8967 |
| 14 | 0 | 14 | 13782.4967 |
| 14 | 1 | 13 | 14121.7043 |
| 15 | 0 | 15 | 14050.9519 |
| 15 | 1 | 15 | 14050.4639[a] |
| 16 | 0 | 16 | 14336.0995 |
| 17 | 1 | 17 | 14638.0818 |
| 17 | 2 | 16 | 15060.1423 |
| 19 | 1 | 19 | 15292.8586 |
| 20 | 0 | 20 | 15646.5620 |
| 21 | 1 | 21 | 16016.2291 |
| 22 | 0 | 22 | 16403.5502 |

(200), as well as the (110) level. Additional assignments have also been sunspot spectra covering both the *L*- and *N*-bands. We are continuing to make progress in assigning the torch spectra.

## Acknowledgments

Financial support for this was provided by The Royal Society, INTAS, the UK Engineering and Physical Science Research Council and Particle Physics and Astronomy Research Council, the NASA astrophysics program, the Canadian Natural Sciences and Engineering Council, the Russian Fund for Fundamental Studies, the Dr. B. Mez-Starck foundation, the Fonds National de la Recherche Scientifique (F.N.R.S., Belgium, F.R.F.C. convention No. 2.4536.01) and the "Actions de Recherches Concertées" (Communauté Française de Belgique). This work was performed as part of IUPAC project number 2004-035-1-100 on "A database of water transitions from experiment and theory."

## Appendix A. Supplementary data

Supplementary data for this article are available on ScienceDirect (www.sciencedirect.com) and as part of the Ohio State University Molecular Spectroscopy Archives (http://msa.lib.ohio-state.edu/jmsa_hp.htm).

## References

[1] P.F. Bernath, Phys. Chem. Chem. Phys. 4 (2002) 1501–1509.
[2] M.C. Cushing, J.T. Rayner, W.D. Vacca, Astrophys. J. 623 (2005) 1115–1140.
[3] L. Wallace, P.F. Bernath, W. Livingston, K. Hinkle, J.R. Busler, B. Guo, K.Q. Zhang, Science 268 (1995) 1155–1158.
[4] O.L. Polyansky, N.F. Zobov, S. Viti, J. Tennyson, P.F. Bernath, L. Wallace, Science 277 (1997) 346–349.
[5] R.J. Barber, J. Tennyson, G.J. Harris, R.N. Tolchenov, Mon. Not. R. Astr. Soc. (accepted for publication).
[6] O.L. Polyansky, A.G. Császár, S.V. Shirin, N.F. Zobov, P. Barletta, J. Tennyson, D.W. Schwenke, P.J. Knowles, Science 299 (2003) 539–542.
[7] J.-M. Flaud, C. Camy-Peyret, J.-P. Maillard, Mol. Phys. 32 (1976) 499–521.
[8] C. Camy-Peyret, J.-M. Flaud, J.-P. Maillard, G. Guelachvili, Mol. Phys. 33 (1977) 1641–1650.
[9] P.-F. Coheur, P.F. Bernath, M. Carleer, R. Colin, O.L. Polyansky, N.F. Zobov, S.V. Shirin, R.J. Barber, J. Tennyson, J. Chem. Phys. 122 (2005) 074307.
[10] N.F. Zobov, S.V. Shirin, O.L. Polyansky, J. Tennyson, P.-F. Coheur, P.F. Bernath, M. Carleer, R. Colin, Chem. Phys. Lett. 414 (2005) 193–197.
[11] R. Colin, P.-F. Coheur, M. Kiseleva, A.C. Vandaele, P.F. Bernath, J. Mol. Spectrosc. 214 (2002) 225–226.
[12] F. Mélen, A.J. Sauval, N. Grevesse, C.B. Farmer, Ch. Servais, L. Delbouille, G. Roland, J. Mol. Spectrosc. 174 (1995) 490–509.
[13] L.S. Rothman, C. Camy-Peyret, J.-M. Flaud, R.R. Gamache, A. Goldman, D. Goorvitch, R.L. Hawkins, J. Schroeder, J.E.A. Selby, R.B. Wattson, HITEMP, the high-temperature molecular spectroscopic database. Private communication.
[14] L. Wallace, W. Livingston, K. Hinkle, P.F. Bernath, Astrophys. J. Suppl. Ser. 106 (1996) 165–169.
[15] N.F. Zobov, O.L. Polyansky, J. Tennyson, S.V. Shirin, R. Nassar, T. Hirao, T. Imajo, P.F. Bernath, L. Wallace, Astrophys. J. 530 (2000) 994–998.
[16] O.L. Polyansky, N.F. Zobov, S. Viti, J. Tennyson, P.F. Bernath, L. Wallace, J. Mol. Spectrosc. 186 (1997) 422–447.
[18] S.V. Shirin, O.L. Polyansky, N.F. Zobov, P. Barletta, J. Tennyson, J. Chem. Phys. 118 (2003) 2124–2129.
[19] D.W. Schwenke, H. Partridge, J. Chem. Phys. 113 (2000) 6592–6597.
[20] J. Tennyson, N.F. Zobov, R. Williamson, O.L. Polyansky, P.F. Bernath, J. Phys. Chem. Ref. Data 30 (2001) 735–831.
[21] O.L. Polyansky, N.F. Zobov, S. Viti, J. Tennyson, P.F. Bernath, L. Wallace, Astrophys. J. 489 (1997) L205–L208.